Available online at www.sciencedirect.com
SCIENCE DIRECT®
Acta Materialia 53 (2005) 4043–4050
Acta MATERIALIA
www.actamat-journals.com

On the evolution of surface roughness during deformation of polycrystalline aluminum alloys

O. Wouters, W.P. Vellinga, R. Van Tijum, J.Th.M. de Hosson *

Department of Applied Physics, Materials Science Centre and the Netherlands Institute for Metals Research, University of Groningen, Nijenborgh 4, 9747 AG Groningen, The Netherlands

Received 31 March 2005; received in revised form 26 April 2005; accepted 5 May 2005
Available online 20 June 2005

Abstract

Surface roughening of polycrystalline Al–Mg alloys during tensile deformation is investigated using white light confocal microscopy. Materials are tested that differ only in grain size. A height–height correlation technique is used to analyze the data. The surface obeys self-affine scaling on length scales up to a correlation length which approximately equals the grain size and above which no height correlation is present. The self-affine scaling exponent increases initially with strain and saturates at a value around 0.9. A linear relation is observed between root-mean-square roughness and both strain and grain size. The observed roughness is explained as the result of the combined effect of a self-affine roughening on a subgrain scale and a grain scale roughening caused by orientation differences between neighboring grains.

Keywords: Aluminum alloys; Orientation imaging microscopy; Surface structure; Tension test; Mesostructure

1. Introduction

Metal surfaces become rough when deformed. This roughness influences not only the appearance of the material but also other surface properties such as reflectivity, lubricant transport, weldability and adhesion. A rough surface may also facilitate the creation of initiation sites for strain localization, which may seriously deteriorate the material mechanical properties. As a consequence, the roughening process has been the subject of numerous investigations, including both experimental and modeling studies. These have shown that the surface roughness depends on strain, grain size and texture. The relationships between roughness and strain and between roughness and grain size are often found to be linear [1,2] but some authors have found deviations from this linear behavior, especially at higher strains [1,3].

Texture was found to have a significant influence on the roughness in several studies [4–10]. Most of these studies are aimed at understanding the development of a typical roping or ridging roughness that is characteristic for rolled highly textured aluminum sheets. Numerical studies [4,6] show that differences in crystallographic orientation, causing differences in hardness and shear incompatibilities between neighboring grains, are a cause for grain scale roughening, which is observed as the typical 'orange peel' surface topography.

This research is aimed at gaining a better understanding of the nature and development of roughness of polycrystalline metal surfaces, which have been deformed by uniaxial tension. In particular we have applied a height–height correlation technique developed to analyze the self-affine nature of grown surfaces. To our current knowledge, a similar approach has been attempted once before by Zaiser et al., who showed that a uniaxially deformed polycrystalline copper sample exhibits a self-affine roughness over a large range in length scales with

* Corresponding author.
E-mail address: j.t.m.de.hosson@rug.nl (J.Th.M. de Hosson).

1359-6454/$30.00
doi:10.1016/j.actamat.2005.05.007

a roughness exponent of approximately 0.75 [11]. One of the great advantages of this technique is that it gives a direct insight into the typical length scales that play a role as the roughness develops. It also makes a distinction possible between values of roughness that are present at different length scales. In this paper, this approach is applied to an extensive data set in order to give a description of a rough surface, which is more powerful in comparison to more conventional methods, which typically provide only root-mean-square (rms) roughness values or make use of pre-defined cut-off frequencies.

2. Experimental method

2.1. Materials and preparation

For our experiments a material is required with a grain size that can be altered without influencing other microstructural features that can affect the material deformation behavior under tension. An Al–8.5%Mg alloy was chosen because its grain size after a recrystallization heat treatment depends strongly on the recrystallization temperature and time and because the magnesium remains in solid solution over a wide range of temperatures. After deforming the material over 80% by cold rolling, four different grain sizes were achieved through recrystallization for 30 min at 350, 400 and 450 °C and for 10 min at 450 °C. Before each new step in the cold rolling process, the material was rotated in order to minimize the occurrence of texture after recrystallization. The resulting grain structures were imaged using orientation imaging microscopy (OIM). Inverse pole figure maps are shown in Fig. 1. The insets show the corresponding (0 0 1) pole figures. Although the number of grains in these scans is insufficient to conduct a thorough texture analysis, they still show that the materials used in this investigation are not strongly textured and that no obvious difference in texture exists between the four different microstructures. The grain size is determined by calculation of the area average:

$$\bar{d} = \frac{\sum_{i=1}^{N} A_i d_i}{\sum_{i=1}^{N} A_i}, \tag{1}$$

where A_i and d_i are the area and diameter of grain i. The grain size values obtained in this way are listed in Table 1.

2.2. Experimental setup

Out of the materials described above, long flat tensile specimens are spark cut eroded with gauge dimensions $28 \times 6.3 \times 1.0$ mm. Before deformation the specimens are polished to a mirror finish. After mounting the specimen in a small portable tensile stage, the stage is mounted in a white light reflection confocal microscope.

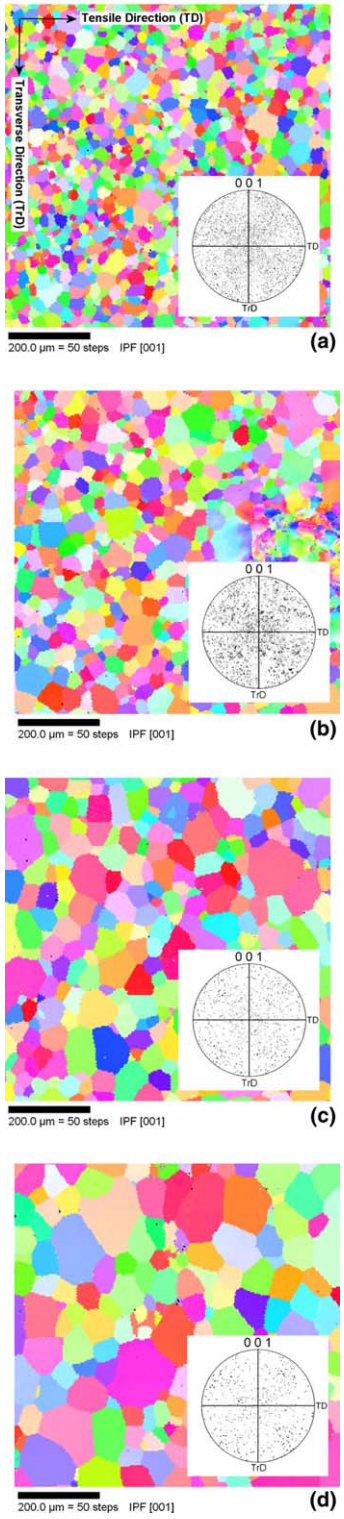

Fig. 1. Orientation imaging microscopy plots of the polished surface of the tensile specimen before deformation showing the differences in grain size after a heat treatment of: (a) 30 min, 350 °C; (b) 30 min, 400 °C; (c) 10 min, 450 °C; and (d) 30 min, 450 °C. The insets show the corresponding (0 0 1) pole figure.

The crosshead speed of the tensile stage is set at 10 μm/s, corresponding to a strain rate of 3.6×10^{-4} s^{-1}. Because of its high lateral and axial resolution, a confocal

Table 1
Grain sizes and heat treatments

Sample	Heat treatment	Grain size (μm)
A	30 min, 350 °C	30.8
B	30 min, 400 °C	44.9
C	10 min, 450 °C	68.1
D	30 min, 450 °C	90.1

microscope is an ideal instrument to acquire topographic information of large surfaces. Using a 20× objective lens, an area of 700 × 660 μm can be scanned with an axial resolution of 40 nm. During the experiments the tensile stage is halted at fixed strains and confocal images are acquired at three positions. Care is taken to ensure that those positions are the same at every measurement in order to be able to accurately study the local roughness evolution with increasing strain.

2.3. Data analysis

To analyze the surface morphology, we have chosen to extract roughness parameters from height–height correlation functions, assuming a partially self-affine scaling behavior [12]. The height–height correlation function

$$g(r) = \frac{1}{L}\int_{-L/2}^{L/2} [h(x+r) - h(x)]^2 \, \mathrm{d}x \tag{2}$$

applied to a matrix of digitized height values takes the form:

$$g(p) = \frac{1}{N_y(N_x - p)} \sum_{l=1}^{N_y} \sum_{n=1}^{N_x - p} [h(p+n, l) - h(n, l)]^2, \tag{3}$$

where N_x and N_y are the dimensions of the height matrix. The correlations are calculated in one direction and averaged over the other.

Assuming a self-affine scaling behavior:

$$h(x) \sim b^{-\alpha} h(bx), \tag{4}$$

where α is the scaling or Hurst exponent, provides a very useful set of parameters to characterize the surface. The height–height correlation function of a self-affine surface takes the form:

$$g(r) = 2w^2 f(r/\xi), \tag{5}$$

where w is the rms width of the height distribution and $f(x)$ is a function that takes the following values:

$$f(x) = x^{2\alpha} \tag{6}$$

for $x \ll 1$ and $f(x) = 1$, for $x \gg 1$. For the height–height correlation function this means:

$$g(r) = mr^{2\alpha} \tag{7}$$

for $r \ll \xi$ and

$$g(r) = 2w^2 \tag{8}$$

for $r \gg \xi$ with $m = 2w^2/\xi^{2\alpha}$. Therefore, plotting the correlation function (Eq. (3)) of a self-affine surface on a double logarithmic scale will result in a straight line with slope 2α, until r is of the order of ξ. At larger values of r, the function will take a constant value of $2w^2$ see Fig. 2. The deviations from the horizontal line towards the end of the curve are a result of the smaller number of height differences that are in the summation of Eq. (3) for higher values of p. To maintain good statistics, correlations are calculated for points with a separation up to 75% of the total profile length.

The heights of points at distances smaller than ξ are correlated, whereas points further apart are uncorrelated. Hence, the parameter ξ is called the correlation length. The scaling parameter α is a measure of this correlation. If the roughness is a result of a random walk displacement, α will be 0.5. Values of α larger than 0.5 indicate a positive correlation, whereas a value smaller than 0.5 means that the heights are anti-correlated. The height images generated by the confocal microscope are flattened before the correlation function is calculated. The correlation function $g(p)$ (the average of the correlation functions of the individual lines) is then plotted on a double logarithmic scale and fitted to the self-affine approximation (Eq. (5)). A linear fit to the first section of the correlation function is used to determine the scaling exponent α. The rms value w is calculated directly from the height data. Finally the correlation length ξ is determined from the intersection of a straight line with slope 2α through the first part of the correlation curve and the horizontal line $g(r) = 2w^2$. The resulting three parameters α, ξ and w completely describe the statistical morphology of the surface within the experimental limits set by the resolution of the confocal microscope.

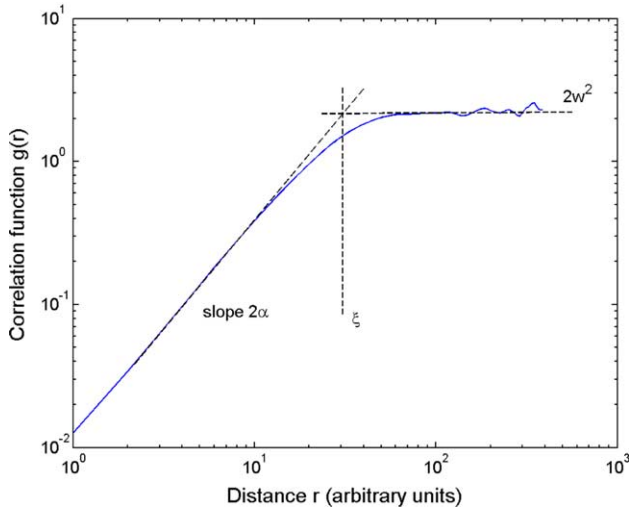

Fig. 2. Height–height correlation function of a self-affine profile created using the Voss-algorithm with $\alpha = 0.8$, $\xi = 30$ and $w = 1$.

Within our work, we focus on the dependence of these parameters with increasing strain and examine the influence of the grain size.

3. Results

Fig. 3 shows the stress–strain curves obtained from the tensile experiments. The small dips in the curves are a result of relaxation at the strains at which the deformation is halted to perform the confocal microscopy. The curves are shown to demonstrate that aside from the grain size the microstructures of the four samples used are identical. They show a slight decrease in yield stress and a slightly higher strain at fracture, but these effects can be related to the increase in grain size.

In Fig. 4, the height–height correlation function for sample A ($\bar{d} = 30.8$ μm) after 12% strain is plotted. The resemblance with the model curve of Fig. 2 is good. The linear first part of the curve indicates a self-affine scaling behavior on smaller length scales. Fig. 5(a) shows the correlation curves for all four samples A–D after 15% straining. With increasing grain size, the curves lie higher and the linear, self-affine regime is longer. Fig. 5(b) shows the curves for sample B ($\bar{d} = 44.9$ μm) for all strain values. The top curve in this graph corresponds to the surface at the largest strain, whereas the bottom curve corresponds to the surface before straining commenced.

Values determined for the scaling parameter α, as obtained by fitting a linear function to the first points in the log–log plots of Fig. 5, are depicted in Fig. 6. For small strains, α is small but it increases with increasing strain, until a constant value of 0.88 ± 0.05 is reached for sample A and of 0.92 ± 0.03 for the samples B, C and D. The error in α for sample A is higher,

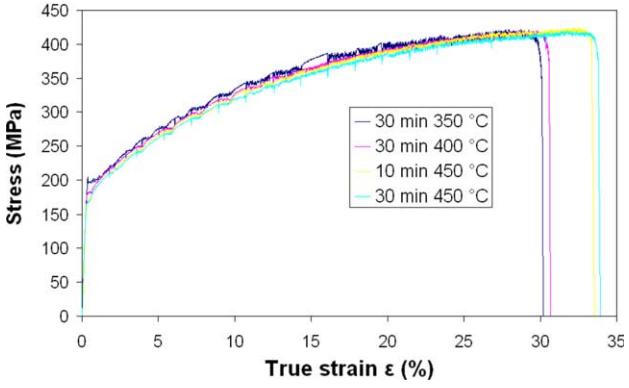

Fig. 3. Stress–strain curves belonging to the four uniaxial tensile experiments.

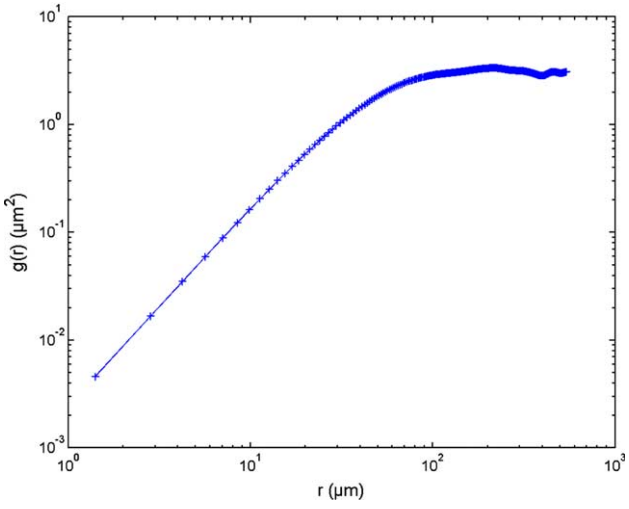

Fig. 4. Experimental height–height correlation function of the sample with the smallest grains after 12% strain.

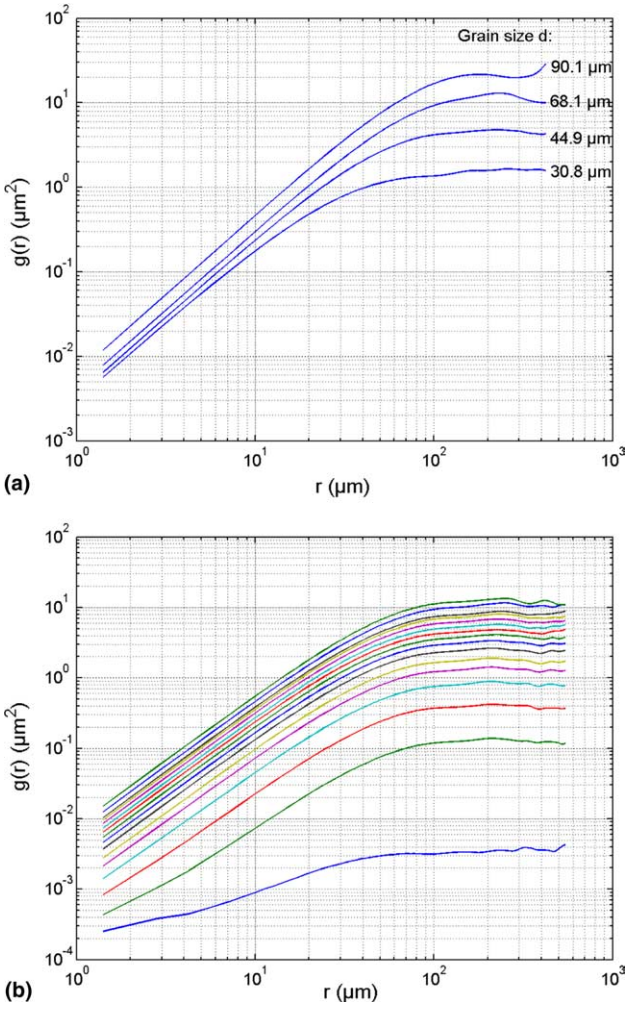

Fig. 5. (a) Height–height correlation functions for all four samples after 15% strain. (b) All correlation curves for the sample with grain size 44.9 μm. Higher curves correspond to measurements performed after a larger strain.

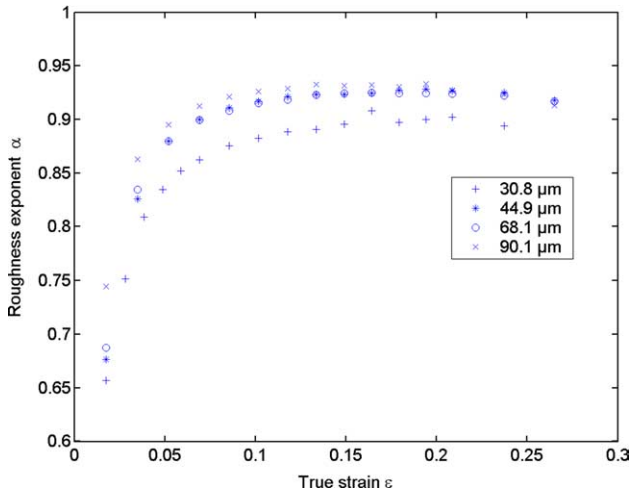

Fig. 6. Roughness parameter α as determined by fitting a straight line to the first few points of the correlation functions.

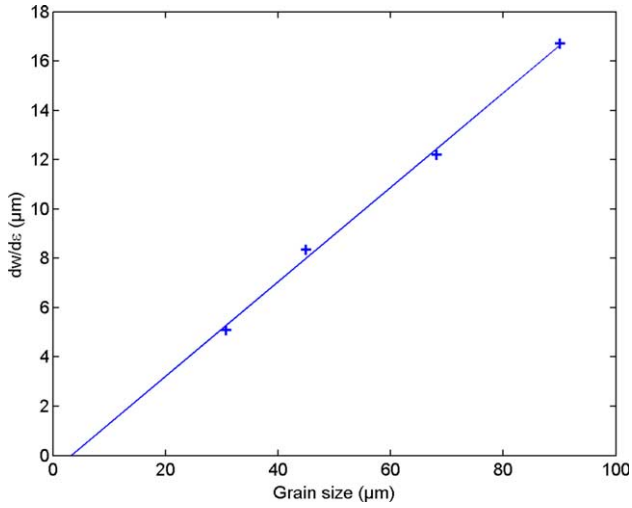

Fig. 8. The slopes dw/dε of the curves in Fig. 7 plotted against the grain size.

because the points in the correlation curve start to deviate from the straight line earlier, making the linear fit less precise.

In Fig. 7 the increase in rms width of the height distribution with increasing strain is plotted. The values for w appear to lie on a straight line. If the slopes of these lines are plotted against the grain size of the corresponding sample material as is done in Fig. 8, it is clear that w scales linearly with both the strain and the grain size as

$$w = 0.19 \cdot \varepsilon \cdot \overline{d}, \tag{9}$$

where ε is the true strain. Finding the intersection of the linear fit through the first section of the correlation function and the line $g(r) = 2w^2$ yields the correlation length ξ. The values for ξ determined for samples A–D are plotted in Fig. 9. Apart from the first few

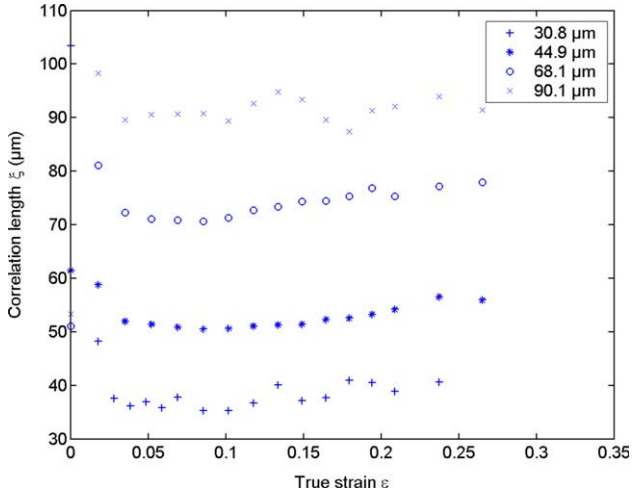

Fig. 9. The correlation length ξ, determined from the fitted α and calculated w-values.

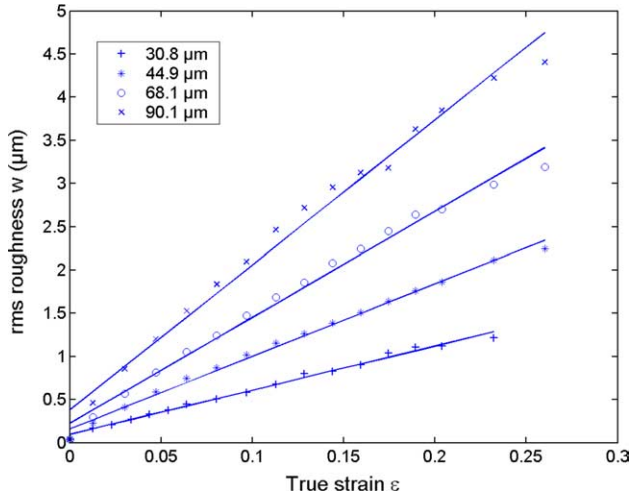

Fig. 7. The rms roughness w scales linear with the strain.

Table 2
Average correlation lengths

Sample	ξ (μm)
A	38
B	52
C	74
D	91

points they are constant. The average values for ξ (excluding the first two points) are listed in Table 2. Based on the accuracy in α and the observed spread in the values of ξ, the accuracy of the values listed in Table 2 are estimated at ±8 μm for sample A and at ±5 μm for samples B, C and D.

In Fig. 10 roughness profiles are shown of a fixed position on the surface of sample A (Fig. 10(a)) and sample

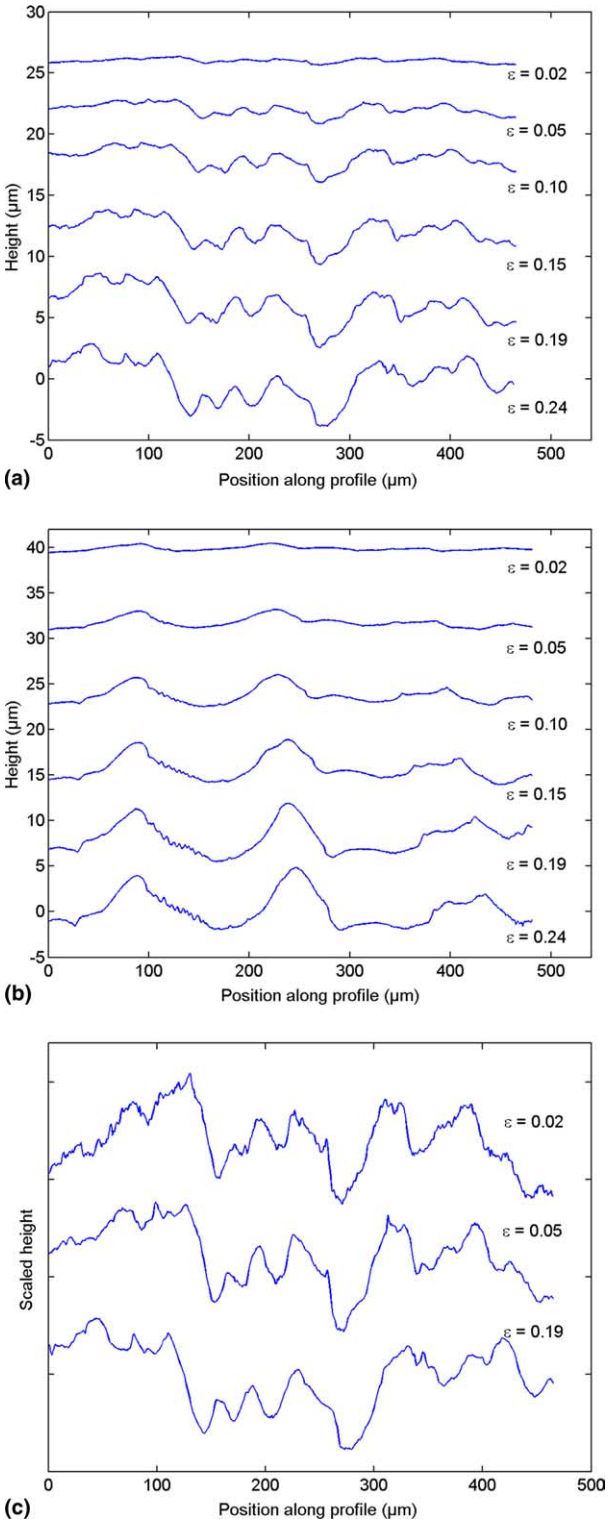

Fig. 10. Local roughness evolution: (a) of the sample with the smallest grains; (b) of the sample with the largest grains; (c) three profiles from (a) rescaled.

D (Fig. 10(b)). In Fig. 10(c) three profiles taken from Fig. 10(a) are scaled vertically so that the shape of the profiles can be compared.

4. Discussion

The striking resemblance between the experimental and theoretical height–height correlation curves justifies the use of this analysis technique. Its power lies in the combined information about large scale roughness (parameter w) and small scale height correlations (roughness exponent α) as well as in the detection of typical lengths at which the roughness develops (correlation length ξ).

The choice of scan size and pixel size can influence the results of a statistical analysis on sampled data quite dramatically. In these measurements care was taken to ensure that the distance between individual sampling points is at least one order of magnitude smaller than the correlation length in order to get a reliable value for the roughness exponent α and to avoid correlation-induced size effects. For determination of the correlation length, a general rule of thumb is to use a scan size, which is at least 10 times larger than the expected value for ξ. This condition is easily met in three out of our four experiments. Due to experimental limitations, the sample with the largest grains shows a correlation length ($\xi = 90$ μm) which is slightly less than 10 times smaller than the scan size (700 μm).

Figs. 7 and 8 show clearly that in these samples the same linear relationship holds between rms roughness and both strain and grain size as was found by other authors. This is a clear indication that roughening is by no means a random process caused by the arbitrary occurrence of dislocation slip steps at the surface. Assuming that the number of steps scales linearly with the strain, this would result in an increase $w \sim \varepsilon^{1/2}$.

Another manifestation of this highly non-random roughening is the high correlation between points at a small length scale resulting in high values for the roughness exponent α (Fig. 9). At the initial stages of straining a high roughness at small length scales develops as is apparent from the low α-values at low strains. This can also be observed in the top profile of Fig. 10(c). This roughness disappears slowly until, after about 10% strain, the small scale roughness remains constant. In effect, although there is a large scale roughening during straining, on a smaller scale the surface is smoothening. By acquiring both the α and w parameters, both effects can be studied simultaneously. In contrast to the rms roughness the small-scale roughness does not seem to depend strongly on the grain size. The α-values for the sample with the smallest grains are a little lower than for the other three samples, but this can be explained by the greater difficulty in determining the correct values as explained above.

From Tables 1 and 2 it is clear that the correlation length ξ can be linked to the grain size. This is reasonable since dislocation mechanisms associated with

plasticity are correlated within grains. Again the relatively large difference between grain size and correlation length for sample A can be explained by the larger error in determining α for this sample. Also the method used to determine the grain size can be open to debate. Here an area average (Eq. (1)), which gives more weight to the larger grains, has been used for two reasons. First, because effectively this also happens when determining the correlation length, and second, to make the grain size determination insensitive to badly indexed points in the OIM scan. These can falsely be interpreted as grains, causing the average grain size to drop.

Combining these results, the determination of the three parameters α, w and ξ leads to the conclusion that, after a certain amount of strain, points within one grain are highly correlated and that these relatively smooth patches are the building blocks for the large scale roughness w. The most striking picture of the non-random manner in which the roughness develops, is given in Fig. 10. When the rescaled profile after just 2% strain is compared to the height profile of the same line after 19% strain, the resemblance is remarkably good, apart from a smoothening on the subgrain scale. All these observations lead to the conclusion that the roughness w is not caused or influenced by microstructural features on a subgrain scale. Of course this holds for roughness within the resolution of the confocal microscope. A more dedicated high-resolution apparatus like an atomic force microscope should be used to study the small-scale roughness and its statistical properties in detail.

The self-affine roughness exponent α found in our experiments is higher than the values obtained by Zaiser et al., who found self-affine behavior in copper alloys with an exponent $\alpha = 0.75$. This difference can be explained by the fact that their measurements were almost completely performed with scan sizes smaller than, or of the order of the grain size, thereby excluding the influence of the roughening mechanism that acts on the grain size scale. This mechanism, which causes the roughness w in our experiments, becomes apparent as large relatively flat facets approximately of the same size as the grains, which can easily be seen in Fig. 10(a) and (b). Adding their effect to the subgrain roughness will result in a value for α closer to 1.

In conclusion, the rms roughness appears to be dominated by microstructural dissimilarities, which manifest themselves on the scale of a grain. In this experiment, the only difference between the grains on this scale is their orientation, or more precisely: the orientation of their slip planes and slip directions with respect to the tensile axis and with respect to the orientation of the neighboring grains. Zhao et al. [4] propose a physical picture of what might happen in these materials. The results of their numerical model show that softer grains or in other words grains which are, due to their orientation, more susceptible to plastic flow, deform more than the harder grains. As a result, these grains, which can also be characterized as having high Schmid or low Taylor factors, stretch more than harder grains. Effectively this causes an inhomogeneous thinning of the material under tensile deformation and an accompanying roughening of the surface. Since the orientation of the grains does not change drastically during straining, this deformation on a grain size scale is a fairly constant process, explaining the linear relationship observed between the roughness w and strain. In a real polycrystalline material the grains are part of a large three dimensional structure comprised of grains with all different orientations. The deformation of a grain will therefore be determined by the combined deformation of its surrounding grains, making the total deformation and resulting surface roughness hard to predict. Further study therefore has to be focused on the relationship between roughness and the orientation of both surface and non-surface grains.

5. Conclusions

Describing the roughness of a deformed metal surface in terms of the statistical parameters α, ξ and w appears to be a good approach to obtaining valuable information about the nature of the roughness and the underlying physical mechanisms.

From these experiments it becomes clear that the roughness on the surface of a deformed polycrystalline aluminum alloy is the combined result of two effects. On a subgrain scale, there is self-affine roughening, the cause of which is not well understood. The correlation length for this self-affine behavior is clearly the grain size of the material. Superimposed on this roughness is a grain scale effect. The origin of this behavior, which causes the rms roughness to scale linearly with both strain and grain size, is found in differences in orientation between neighboring grains. Softer grains will deform more than harder grains, causing an inhomogeneous thinning of the material during tensile deformation and effectively also a grain scale roughness on the surface.

Acknowledgement

The work is part of the research program of the Foundation of Fundamental Research on Matter (FOM-Utrecht) and has been made possible by financial support from the Netherlands Organization for Research (NWO-The Hague), the Netherlands Institute for Metals Research, the Foundation for Technical Sciences and the Innovative Research Program (IOP-Senter, The Hague).

References

[1] Wilson DV, Roberts WT, Rodrigues PMB. Metall Trans A 1981;12:1595.
[2] Mahmudi R, Mehdizadeh M. J Mater Proc Technol 1998;80–81:707.
[3] Mizuno T, Mulki H. Wear 1996;198:176.
[4] Zhao Z, Radovitzky R, Cuitiño A. Acta Mater 2004;52:5791.
[5] Lee PS, Piehler HR, Adams BL, Jarvis G, Hampel H, Rollett AD. J Mater Proc Technol 1998;80–81:315.
[6] Becker R. Acta Mater 1998;46(4):1385.
[7] Wittridge NJ, Knutsen RD. Mater Sci Eng A 1999;269:205.
[8] Raabe D, Sachtleber M, Weiland H, Scheele G, Zhao Z. Acta Mater 2003;51:1539.
[9] Wilson DV, Roberts WT, Rodrigues PMB. Metall Trans A 1981;12:1603.
[10] Baczynski GJ, Guzzo R, Ball MD, Lloyd DJ. Acta Mater 2000;48:3361.
[11] Zaiser M, Madani F, Koutsos V, Aifantes EC. Phys Rev Lett 2004;93(19):195507.
[12] Zhao Y, Wang GC, Lu TM. Characterization of amorphous and crystalline rough surface: principles and applications. London: Academic Press; 2001.